Egyptian Journal of Aquatic Biology & Fisheries
Zoology Department, Faculty of Science,
Ain Shams University, Cairo, Egypt.
ISSN 1110 – 6131
Vol. 27(5): 411 – 427 (2023)
www.ejabf.journals.ekb.eg

A Simplified 3D Model for Remediation of Pollution in a River by Releasing Clean Water Using the Advection-Dispersion Equation

Ahmed Saleh [1], Mourad F. Dimian [2] and Fayez N. Ibrahim [2,*]

[1] Egyptian Academy for Engineering and Advanced Technology, Department of Basic Science, Cairo, Egypt.

[2,*] Ain Shams University, Faculty of Science, Department of Mathematics, Cairo, Egypt.

[*]**Corresponding Author: fayeznasif@yahoo.co.uk**

ARTICLE INFO

Article History:
Received: Sept. 1, 2023
Accepted: Sept. 24, 2023
Online: Sept. 30, 2023

Keywords:
Remediation of water pollution, dimensionless variables, advection-dispersion equation, finite difference method, Laplace transformation.

ABSTRACT

An analytical solution is obtained for the three-dimensional advection-dispersion equation describing temporally dependent flow domain through an isotropic semi-infinite homogeneous porous medium by using the Laplace transformation technique. Also, a numerical solution is obtained by using the explicit finite difference method. The usage of dimensionless variables allows this solution to be applicable in a wide variety of cases. Impacts of different parameters controlling pollutant dispersion are studied with the help of graphs and a table. We discuss how to use the fact that the provided solution predicts pollutant concentration along the river to help in the decision-making regarding its remediation with effective methods. This paper mathematically indicates that releasing clean water from a barrage reduces the pollutant concentration in a river.

INTRODUCTION

Pollution is one of the hard challenges that face our societies in the current era. Water pollution is specifically a threatening one as it affects the main source of life causing damage to humans and the environment. We recall that water pollution is defined by the contamination of natural water bodies by chemical, physical, radioactive or pathogenic microbial substances. Thus, remediation of pollution of water resources is of high demand. A mathematically simple way to model this situation is to use the Advection-Dispersion Equation (ADE). The ADE describes the solute transport due to the combined effects of dispersion and groundwater flow in porous media **(Bear and Verruijt, 1987)**. Also, the ADE is employed in chemical engineering **(Bérard *et al.*, 2020)** and in modelling various situations, including radionuclide releases **(Esmail *et al.*, 2020)**, secondary migration of hydrocarbons **(Borazjani *et al.*, 2019)**, the dispersion of air pollutants in a finite media **(Sylvain *et al.*, 2021)**, petroleum contamination **(Berlin and Suresh, 2019)**, among many others. It is obvious that a dimensionless solution accounting for different cases is of great value.

The analytical solutions of the ADE exist for a wide range of cases as early as the 1980s. Those are easily found in the literature. We present in this paragraph some of the recent developments. **(Yadav and Kumar, 2017)** obtained analytical solutions for the 2D ADE with pulse-type input source**. (Olowe and Kumarasamy, 2017)** simulated ammonia nutrient pollutant transport using the ADE and Hybrid Cell in Series models. **(Chaudhary *et al*., 2020)** analysed the 1D pollutant transport in semi-infinite groundwater reservoir. **(Manitcharoen and Pimpunchat, 2020)** obtained analytical and numerical solutions to the 1D ADE for uniformly and exponentially increasing forms of sources. **(Yadav and Kumar, 2021)** obtained analytical solution of two-dimensional conservative solute transport in a heterogeneous porous medium for varying input point source. **(Saleh *et al*., 2022)** solved the 1D ADE describing exponential variations in pollutant concentration numerically and analytically capturing results regarding the remediation of pollution. **(Hadhouda and Hassan, 2022)** solved numerically the coupled pair of nonlinear equations modelling pollutant concentration and dissolved oxygen concentration obtaining results concerning the unsteady remediation of pollution in a river by aeration with the release of clean water.

In the present paper, we introduce dimensionless variables and acquire analytical and numerical solutions in the dimensionless form for the 3D ADE with temporally dependent parameters using the Laplace transform and the explicit finite difference scheme respectively. We compare the analytical solution with the respective numerical solution. Furthermore, we investigate 3 cases: (i) The effect of releasing water whose pollutant concentration is less than the river's initial pollutant concentration. (ii) The effect of releasing water whose pollutant concentration is more than the river's initial pollutant concentration. (iii) The case study of pulse-type input condition. By using the table and figures we explain how this simple model can predict pollutant concentration values at a given time and place along a river. Resulting in a big control and flexibility over different treatment methods (engineering, chemical, biological, …etc) which leads to efficient management of water resources.

MATERIALS AND METHODS

1. The Governing Equation:

The three-dimensional partial differential equation describing hydrodynamic dispersion in adsorbing homogenous, isotropic porous medium can be written as **(Bear, 1972; Leij *et al*., 1991; Yadav *et al*., 2010)**:

$$R\frac{\partial C}{\partial t} = D_x(t)\frac{\partial^2 C}{\partial x^2} + D_y(t)\frac{\partial^2 C}{\partial y^2} + D_z(t)\frac{\partial^2 C}{\partial z^2} - u(t)\frac{\partial C}{\partial x} - v(t)\frac{\partial C}{\partial y} - w(t)\frac{\partial C}{\partial z} - \gamma(t)C, \qquad (1)$$

where R is the retardation factor, $C(x, y, z, t)$ (kg m^{-3}) is the pollutant concentration for a porous medium. $D_x(t)$ (m^2 day^{-1}), $D_y(t)$ (m^2 day^{-1}) and $D_z(t)$ (m^2 day^{-1}) are the dispersion coefficients in the x (m), y(m) and z(m) directions respectively. $u(t)$ (m day^{-1}), $v(t)$ (m day^{-1}) and $w(t)$ (m day^{-1}) are flow velocities in the x, y and z directions respectively, $\gamma(t)$

(day^{-1}) is a first-order decay term, each of them is a function of time t (day). z is positive downwards, where the origin is taken to be on the surface of the river.

The flow domain parameters are considered to be temporally dependent and the solute dispersion coefficients are considered to vary proportionally to the respective velocity **(Singh *et al*., 2013)**, so we have:

$$\left.\begin{aligned} &u(t) = u_0 f(mt), v(t) = v_0 f(mt),\ w(t) = w_0 f(mt), \gamma(t) = \gamma_0 f(mt),\\ &D_x(t) = D_{x_0} f(mt), D_y(t) = D_{y_0} f(mt),\ D_z(t) = D_{z_0} f(mt), \end{aligned}\right\} \quad (2)$$

where u_0 (m day^{-1}), v_0 (m day^{-1}) and w_0 (m day^{-1}) are the initial velocity components. $D_{x_0} = au_0$ (m^2 day^{-1}), $D_{y_0} = av_0$ (m^2 day^{-1}) and $D_{z_0} = aw_0$ (m^2 day^{-1}) are the initial dispersion coefficients. γ_0 (day^{-1}) is the first-order decay constant term. m (day^{-1}) is a constant. a (m) is a constant that depends upon pore geometry of the medium. We choose $f(mt)$ such that for $t = 0$ or $m = 0$ we have $f(mt) = 1$ which ensures that the nature of the initial condition doesn't change in the new time domain. Introducing a distance variable χ (m) and a time variable T (day) defined by **(Crank, 1975; Jaiswal *et al*., 2009; Kumar *et al*., 2011; Yadav *et al*., 2011)**:

$$\chi = x + y\sqrt{\frac{D_{y_0}}{D_{x_0}}} + z\sqrt{\frac{D_{z_0}}{D_{x_0}}}\ ,\ \ T = \int_0^t \frac{f(mt)}{R}\, dt. \quad (3)$$

Equations (2) and (3) transform equation (1) into:

$$\frac{\partial C}{\partial T} = D_0 \frac{\partial^2 C}{\partial \chi^2} - U\ \frac{\partial C}{\partial \chi} - \gamma_0 C. \quad (4)$$

Where $D_0 = D_{x_0}\left(1 + \frac{D^2{y_0}}{D^2{x_0}} + \frac{D^2{z_0}}{D^2{x_0}}\right)$, $U = \left(u_0 + v_0\sqrt{\frac{D_{y_0}}{D_{x_0}}} + w_0\sqrt{\frac{D_{z_0}}{D_{x_0}}}\right)$. (5)

Such that D_0 represents the dispersion and U represents the velocity.

2. Problem description:

We assume a point source input at the origin C_0 , with initial concentration along the river C_1. Also, far from the source, it is assumed that there is no pollutant concentration exchange with the system. Hence the initial and boundary conditions are:

$$C(x,y,z,t) = C_1 \quad , \quad x \geq 0\ , y \geq 0\ , z \geq 0\ , \quad t = 0, \quad (6)$$

$$C(x,y,z,t) = C_0 \quad , \quad x = 0\ , y = 0\ , z = 0\ , \quad t > 0, \quad (7)$$

$$\frac{\partial C}{\partial x} = \frac{\partial C}{\partial y} = \frac{\partial C}{\partial z} = 0\ , \quad x \to \infty\ , y \to \infty , z \to \infty , \quad t \geq 0. \quad (8)$$

Equation (3) transforms equations (6-8) into:

$$C(\chi,T) = C_1 \quad ,\chi \geq 0 \ , \quad T = 0, \tag{9}$$

$$C(\chi,T) = C_0 \quad ,\chi = 0 \ , \quad T > 0, \tag{10}$$

$$\frac{\partial C}{\partial \chi} = 0 \qquad ,\chi \to \infty \, , \quad T \geq 0. \tag{11}$$

From equations (4), (6), and (7), we see that the pollutant concentration C in the porous media depends on the five parameters (D_0, U, γ_0, C_1 and C_0). It is generally more convenient to write equations in dimensionless variables. Take γ_0 as the time scale, u_0 as the velocity scale, C_0 as the concentration scale and use the symbol (*) to denote a dimensionless quantity, hence:

$$C^* = \frac{C}{C_0} \quad , \quad C_1^* = \frac{C_1}{C_0} \quad , C_0^* = 1 \, , \quad T^* = T\,\gamma_0 \quad , \quad U^* = \frac{U}{u_0} \quad , \quad \chi^* = \frac{\chi\,\gamma_0}{u_0} \,. \tag{12}$$

Equation (12) transforms equations (4) and (9 -11) into:

$$\frac{\partial C^*}{\partial T^*} = \frac{1}{Pe}\,\frac{\partial^2 C^*}{\partial \chi^{*2}} - U^*\frac{\partial C^*}{\partial \chi^*} - C^*, \tag{13}$$

$$C^*(\chi^*,T^*) = C^*{}_1 \qquad , \quad \chi^* \geq 0 \qquad ,T^* = 0, \tag{14}$$

$$C^*(\chi^*,T^*) = 1 \qquad , \quad \chi^* = 0 \qquad ,T^* > 0, \tag{15}$$

$$\frac{\partial C^*}{\partial \chi^*} = 0 \qquad , \quad \chi^* \to \infty \qquad ,T^* \geq 0, \tag{16}$$

where $Pe = \frac{{u_0}^2}{D_0\,\gamma_0}$ is the Peclet number. From equations (13-16) it is clear that:

(I) The parameters controlling C^* are reduced from five (D_0, U, γ_0, C_1 and C_0) to the three ($Pe, U^*$and C_1^*).

(II) The effect of ${u_0}^2$ is opposite to the effect of $D_0\,\gamma_0$ on C^*.

(III) The effect of γ_0 is the same as the effect of D_0 on C^*.

To solve equation (13) associated with initial and boundary conditions (14-16), we use the following transformation **(Kumar *et al*., 2011)** which eliminates the convection term and the first order decay term:

$$C^*(\chi^*,T^*) = K(\chi^*,T^*)\ \exp\left(\frac{U^*Pe}{2}\chi^* - \alpha T^*\right), \tag{17}$$

where $\alpha = \left(\frac{U^{*2}Pe}{4} + 1\right)$. Hence equation (17) transforms equations (13-16) into:

$$\frac{\partial K}{\partial T^*} = \frac{1}{Pe}\,\frac{\partial^2 K}{\partial \chi^{*2}}, \tag{18}$$

$$K(\chi^*,T^*) = C_1^* \exp\left(-\frac{U^*Pe}{2}\chi^*\right) \quad , \qquad \chi^* \geq 0 \quad , \quad T^* = 0, \tag{19}$$

$$K(\chi^*,T^*) = exp(\alpha\, T^*) \qquad , \qquad \chi^* = 0 \quad , \quad T^* > 0, \tag{20}$$

$$\frac{\partial K}{\partial \chi^*} = -\frac{U^*Pe}{2}\ K \qquad , \qquad \chi^* \to \infty \quad , \quad T^* \geq 0. \tag{21}$$

3. Analytical solution of the problem:

Applying Laplace transformation on equations (18, 20 and 21) and using equation (19), then we have:

$$\frac{1}{Pe}\ \frac{d^2\bar{K}(\chi^*,p)}{d\chi^{*2}} - p\bar{K}(\chi^*,\ p) = -C_1^*\, exp\left(-\frac{U^*Pe}{2}\chi^*\right), \tag{22}$$

$$\bar{K}(\chi^*,p) = \frac{1}{p-\alpha}\quad,\quad \chi^* = 0, \tag{23}$$

$$\frac{d\bar{K}}{d\chi^*} = -\frac{U^*Pe}{2}\ \bar{K}\quad,\quad \chi^* \to \infty, \tag{24}$$

where p is the Laplace transformation parameter. The general solution of equation (22) with boundary conditions (23) and (24) is given by:

$$\bar{K}(\chi^*,\ p) = \left\{\left(\frac{1}{p-\alpha}\right) - \frac{C_1^*}{(p-\beta^2)}\right\}\cdot\ exp\left(-\sqrt{Pe\ p}\chi^*\right) + \frac{C_1^*}{(p-\beta^2)}\cdot exp\left(-\frac{U^*Pe}{2}\chi^*\right). \tag{25}$$

Now, applying the inverse of Laplace transformation on equation (25) and using equation (17), hence the analytical solution of the ADE (13) associated with the initial and boundary conditions (14-16) may be written in terms of $(\chi^*,\ T^*)$ as:

$$C^*(\chi^*,\ T^*) = C_1^*\ exp(-T^*)\left\{\begin{matrix} 1 - \frac{1}{2}\ erfc\left(\frac{\sqrt{Pe}(\chi^* - U^*T^*)}{2\sqrt{T^*}}\right) - \\ \frac{1}{2}\ exp(U^*Pe\chi^*)\ erfc\ \left(\frac{\sqrt{Pe}(\chi^* + U^*T^*)}{2\sqrt{T^*}}\right)\end{matrix}\right\}$$

$$+\frac{1}{2}\ exp[\sqrt{Pe}\left(\beta - \sqrt{\beta^2+1}\right)\ \chi^*]\ erfc\ \left(\frac{\sqrt{Pe}\left(\chi^* - \sqrt{U^{*2} + \frac{4}{Pe}\ T^*}\right)}{2\sqrt{T^*}}\right)$$

$$+\frac{1}{2}\ \exp[\sqrt{Pe}\left(\beta + \sqrt{\beta^2+1}\right)\ \chi^*]\ erfc\ \left(\frac{\sqrt{Pe}\left(\chi^* + \sqrt{U^{*2} + \frac{4}{Pe}\ T^*}\right)}{2\sqrt{T^*}}\right), \tag{26}$$

where $\beta^2 = \frac{U^{*2}Pe}{4}$. We confirmed that equation (26) satisfies equations (13-16).

4. Special Cases:

4.1 Releasing water whose pollutant concentration is higher than the river's pollutant concentration (i.e. $C_0^* > C_1^* = 0$):

This case is derived from equation (26) as:

$C^*(\chi^*,\ T^*) =$

$\frac{1}{2}\ exp[\sqrt{Pe}\left(\beta - \sqrt{\beta^2+1}\right)\chi^*]\ erfc\ \left(\frac{\sqrt{Pe}\left(\chi^* - \sqrt{U^{*2}+\frac{4}{Pe}T^*}\right)}{2\sqrt{T^*}}\right) +$

$\frac{1}{2}\ \exp[\sqrt{Pe}\left(\beta + \sqrt{\beta^2+1}\right)\chi^*]\ erfc\ \left(\frac{\sqrt{Pe}\left(\chi^* + \sqrt{U^{*2}+\frac{4}{Pe}T^*}\right)}{2\sqrt{T^*}}\right).$ (27)

This equation is equivalent to that obtained by **(Genuchten and Alves, 1982)** (Problem C13, R= μ =1, C_a=C_0^*, $C_b = 0$, γ=0).

4.2 Pulse-type input condition:

We consider equation (13) with pulse-type input condition:

$$C(\chi, T) = C_1 \quad , \quad \chi \geq 0 \quad , \quad T = 0, \tag{28}$$

$$C(\chi, T) = \begin{cases} C_0 & , \quad \chi = 0 \quad , \quad 0 < T \leq T_0 \\ 0 & , \quad \chi = 0 \quad , \quad T > T_0 \end{cases} \tag{29}$$

$$\frac{\partial C}{\partial \chi} = 0 \quad , \quad \chi \to \infty \quad , \quad T \geq 0. \tag{30}$$

Using dimensionless variables defined in equation (12), then equations (28-30) give:

$$C^*(\chi^*, T^*) = C^*{}_1 \quad , \quad \chi^* \geq 0 \quad , \quad T^* = 0, \tag{31}$$

$$C^*(\chi^*, T^*) = \begin{cases} 1 & , \quad \chi^* = 0 \quad , \quad 0 < T^* \leq T^*{}_0\,, \\ 0 & , \quad \chi^* = 0 \quad , \quad T^* > T^*{}_0\,, \end{cases} \tag{32}$$

$$\frac{\partial C^*}{\partial \chi^*} = 0 \quad , \quad \chi^* \to \infty \quad , \quad T^* \geq 0. \tag{33}$$

The solution of equation (13) subjected to initial and boundary conditions (31-33) is given by **(Genuchten and Alves, 1982)** (Problem C5, R=μ=1, γ=0) as:

For $0 < T^* \leq T^*{}_0\,,$

$$C^*(\chi^*,\ T^*) = C_1^*\,exp(-T^*)\left\{\begin{matrix} 1 - \frac{1}{2}\ erfc\left(\frac{\sqrt{Pe}(\chi^* - U^*T^*)}{2\sqrt{T^*}}\right) - \\ \frac{1}{2}\ exp(U^*Pe\chi^*)\ \ erfc\ \left(\frac{\sqrt{Pe}(\chi^* + U^*T^*)}{2\sqrt{T^*}}\right) \end{matrix}\right\} +$$

$$+\frac{1}{2}\ \exp\left[\left(\frac{Pe\left(U^*-U^*\sqrt{1+\frac{4}{Pe\,U^{*2}}}\right)}{2}\right)\ \chi^*\right]\ erfc\ \left(\frac{\sqrt{Pe}\left(\chi^*-U^*\sqrt{1+\frac{4}{Pe\,U^{*2}}}\,T^*\right)}{2\sqrt{T^*}}\right)+$$

$$\frac{1}{2}\ \exp\left[\left(\frac{Pe\left(U^*+U^*\sqrt{1+\frac{4}{Pe\,U^{*2}}}\right)}{2}\right)\ \chi^*\right]\ erfc\ \left(\frac{\sqrt{Pe}\left(\chi^*+U^*\sqrt{1+\frac{4}{Pe\,U^{*2}}}\,T^*\right)}{2\sqrt{T^*}}\right). \tag{34}$$

For $T^* > {T^*}_0$,

$$C^*(\chi^*,\ T^*) = C_1^*\ exp(-T^*)\begin{Bmatrix} 1-\frac{1}{2}\ erfc\left(\frac{\sqrt{P}(\chi^*-U^*T^*)}{2\sqrt{T^*}}\right)- \\ \frac{1}{2}\ exp(U^*Pe\chi^*)\ \ erfc\ \left(\frac{\sqrt{Pe}(\chi^*+U^*T^*)}{2\sqrt{T^*}}\right)\end{Bmatrix}+$$

$$\frac{1}{2}\ \exp[\frac{Pe\left(U^*-U^*\sqrt{1+\frac{4}{Pe\,U^{*2}}}\right)}{2}\ \chi^*]\ erfc\ \left(\frac{\sqrt{Pe}\left(\chi^*-U^*\sqrt{1+\frac{4}{Pe\,U^{*2}}}\,T^*\right)}{2\sqrt{T^*}}\right)+$$

$$\frac{1}{2}\ \exp[\frac{Pe\left(U^*+U^*\sqrt{1+\frac{4}{Pe\,U^{*2}}}\right)}{2}\ \chi^*]\ erfc\ \left(\frac{\sqrt{Pe}\left(\chi^*+U^*\sqrt{1+\frac{4}{Pe\,U^{*2}}}\,T^*\right)}{2\sqrt{T^*}}\right)-$$

$$\frac{1}{2}\ \exp\left[\frac{Pe\left(U^*-U^*\sqrt{1+\frac{4}{Pe\,U^{*2}}}\right)}{2}\ \chi^*\right]\ erfc\ \left(\frac{\sqrt{Pe}\left(\chi^*-U^*\sqrt{1+\frac{4}{Pe\,U^{*2}}}\,(T^*-{T^*}_0)\right)}{2\sqrt{T^*-{T^*}_0}}\right)-$$

$$\frac{1}{2}\ ex\,p\left[\frac{Pe\left(U^*+U^*\sqrt{1+\frac{4}{Pe\,U^{*2}}}\right)}{2}\ \chi^*\right]\ erfc\ \left(\frac{\sqrt{Pe}\left(\chi^*+U^*\sqrt{1+\frac{4}{Pe\,U^{*2}}}\,(T^*-{T^*}_0)\right)}{2\sqrt{T^*-{T^*}_0}}\right). \tag{35}$$

5. Numerical solution:

It is known that analytical solutions of ADE with limited initial and boundary conditions have very few applications and are very lengthy. Numerical methods do not have such limitations especially for arbitrary conditions **(Savovic and Djordjevich, 2012)**. Hence, numerical solutions are also obtained using a two-level explicit finite difference scheme in the case of uniform input. Step-size $\Delta\chi^*$=0.1 and ΔT^*=0.002 along χ^*-domain and T^*-domain, are chosen respectively. The explicit finite difference method is applied to solve equation (13) with initial and boundary conditions (14-16). The central difference scheme was used to represent $\frac{\partial^2 C^*}{\partial \chi^{*2}}$ *and* $\frac{\partial C^*}{\partial \chi^*}$ and a forward difference scheme for the term $\frac{\partial C^*}{\partial T^*}$, with these substitutions, equation (13) can be written as:

$$C^*_{i,j+1} = r_1 C^*_{i+1,j} +\ r_2 C^*_{i,j} + r_3 C^*_{i-1,j}\ , \tag{36}$$

where i and j refer to the discrete step lengths $\Delta\chi^*$and ΔT^* for the coordinates $\chi^*$and T^* respectively, and $r_1 = \frac{\Delta T^*}{Pe\ (\Delta\chi^*)^2} - \frac{U^*\ \Delta T^*}{2\ \Delta\chi^*}$, $r_2 = 1 - \frac{2\ \Delta T^*}{Pe\ (\Delta\chi^*)^2} - \Delta T^*$, $r_3 = \frac{\Delta T^*}{Pe\ (\Delta\chi^*)^2} + \frac{U^*\ \Delta T^*}{2\ \Delta\chi^*}$. The stability criterion: r_1, r_2, r_3 are chosen to lie between 0.0 and 0.5. Equation (36) represents a formula for $C^*_{i,j+1}$ at the $(\mathrm{i},\mathrm{j}+1)^{th}$ mesh point in terms of known values along the j^{th} time row. The initial and boundary conditions (14-16) may be written in the finite difference form as:

$$C^*_{i,0} = C^*_1 \qquad , \quad \chi^* \geq 0 \qquad , T^* = 0, \tag{37}$$

$$C^*_{0,j} = 1 \qquad , \quad \chi^* = 0 \qquad , T^* > 0, \tag{38}$$

$$C^*_{N,j} = C^*_{N-1,j} \qquad , \quad \chi^* \geq 0 \qquad , T^* = 0, \tag{39}$$

where $N = \chi^*_\infty / \, \Delta\chi^*$ is the grid dimension in the χ^*direction and χ^*_∞ is the distance measured from the origin at which $\frac{\partial C^*}{\partial \chi^*} \to 0$.

RESULTS AND DISCUSSION

We set $f(mt) = exp(-m\,t)$.The solutions obtained are illustrated in **Table 1** and **Figs. 1-8**. **Table 1** shows the values of C^* for the common values used in **Table 1** and **Figs. 1,2**: $\mathrm{u}_0 = 1.05$ (md^{-1}), $\mathrm{v}_0 = 0.105(\mathrm{md}^{-1})$, $\mathrm{w}_0 = 0.095(md^{-1})$, $a = 1.1905(\mathrm{m})$, $R = 1$, $m = 0.01(\mathrm{d}^{-1})$, $\gamma_0 = 0.1(\mathrm{d}^{-1})$, U^*=1.06 and C^*_1=0.1. **Fig. 1** displays the variation of C^* with time T^* for the values $T^* = 0.049875\ and\ 0{,}14888$, which corresponds to t = 0.5 and 1.5 (day) respectively, $0 \leq x \leq 1(m)$,$0 \leq y \leq 1(m)$, z = 0(m), $Pe = 8.467$. From **Fig. 1** and **Table 1** It is clear that C^* increases as time T^* increases at any point of the domain as expected. This result agrees with that obtained by **(Dimian *et al*., 2013; Dimian *et al*., 2014; Wadi *et al*., 2014; Ibrahim *et al*., 2015; Yadav and Kumar, 2021).**

Fig. 2 illustrates the variation of C^* with Peclet number Pe for the values Pe = 2, 10; $0 \leq x \leq 1(m)$,$0 \leq y \leq 1(m)$, z = 0(m), and T^*=0.15. From **Fig. 2** and **Table 1** It is clear that C^* decreases with the increase of the Peclet number (Pe) at any point of the domain i.e. with the increase of u_0 or the decrease of either D_0 or γ_0. This result agrees with that obtained by **(Chrysikopoulos *et al*., 1990)**.

Fig. 3 shows a comparison between the analytical solution (given by equation (26)) and the numerical solution of equation (36), for the values $0 \leq \chi^* \leq 1$, $T^* = 0.15$, $Pe = 8.467$, U^*=1.06 and C^*_1=0.1. Clearly, a complete agreement is found. Also, from the data in **Table 1** and **Fig. 3**, for constant values of *x*, *y* and increasing values of *z*, i.e. increasing values of χ^*, the values of C^* decrease and remain constant as $\chi^* \to \chi^*_\infty$ which confirms the boundary condition $\frac{\partial C^*}{\partial \chi^*} \to 0$.

Fig. 4 illustrates the variation of C^* with C^*_1, for the values C^*_1= 1.5, 1.75, 2; $0 \leq \chi^* \leq 1$, Pe=8.467, U^*=1.06 and T^*=0.15. We observe that:

1- Near the pumping origin (χ^*=0) where the pollutant concentration of the released water ($C^*_0 = 1$) is less than the river's initial pollutant concentration (C^*_1), the effect of C^*_0 is dominant, and as χ^*increases, the effect of C^*_0 decreases and the effect of C^*_1 is dominant.

2- The pollutant concentration takes an intermediate value between C_0^* and C_1^*. This confirms that releasing clean water into the river (i.e. $C_0^* < C_1^*$) decreases the pollutant concentration of the river.

Figs. 5,6 display the variation of $C^*$with T^* for the pulse-type input case for the values $0 \leq \chi^* \leq 1$ (**Fig. 5**), $0 \leq \chi^* \leq 5$ (**Fig. 6**) , Pe=8.467, U^*=1.06, C_1^*=0.1 and ${T^*}_0$=0.5 and T^*=0.1, 0.2, 0.3, 0.7, 0.8 and 0.9. It is clear that if $T^* < {T^*}_0$ and $C_0^* > C_1^*$, as time increases the value of C^* increases at any given point, and if $T^* > {T^*}_0$ and $C_0^* < C_1^*$, as time increases the value of C^* decreases at any given point. Using **Fig. 6**, we can predict with accuracy the time and the position of the peak of the curve which represents the place of accumulation of pollutants in the river, and by doing so we allow for various methods (chemical for example) to be very effective in treating pollution in a relatively small area of the river at a reasonable time.

Fig. 7 shows the variation of C^* with U^* for the pulse-type input case at $T^* > {T^*}_0$ for the values $0 \leq \chi^* \leq 8$, Pe=8.467, C_1^*=0.1>C_0^*, T^*=0.75 and ${T^*}_0$=0.5 where U^*= 2, 4, 6 and 8. Since the flux Q of water (i.e. the volume of water crossing a section of area A of a river) Q = $A\ U^*$, hence the flux Q increases as U^* increases. It is clear that as U^* increases the maximum value of C^* decreases. Furthermore, as U^* increases, the cleaned distance measured from the origin (χ^*=0) increases. It is noticed that for high values of U^*, the value C^*fluctuates before settling for the constant value, this is due to the accumulation of pollutants cleaned and transported from the closest points to the barrage.

Comparing this figure with the experimental data given by **(El Shazely, 2006)**, we notice that:
In figure (3) in the experimental data, when the volume of released water increases from 10 to 30 million m^3/day i.e. it increased 3 times, the peak of the curve (maximum concentration of the pollution) decreases to roughly 50%. Also, in **Fig. 7** in this study when U^* increases 3 times (for example from 2 to 6) the corresponding peak is reduced to about 50% as well.

Fig. 8 shows the variation of C^* with Pe for $T^* > {T^*}_0$ in the pulse-type input case for the values $0 \leq \chi^* \leq 3$, $U^* = 1.06$, C_1^*=0.1, T^*=0.75 and ${T^*}_0$=0.5 where Pe = 8.467, 24 and 72. It is clear that C^* increases as the value of Pe increases. This result agrees with that obtained by **(Chrysikopoulos *et al*., 1990)**. From **Figs. 2,8** we conclude that the variation of C^* with Pe depends on the relative pollutant concentration between the released water (C_0^*) and the river's (C_1^*).

Table (1): The variation of C^* with z(m), t(day), and Pe for the values $R = 1, m = 0.01(\mathrm{d}^{-1}), U^*$=1.06, C_1^*=0.1.

x	y	z	t	Pe	C^*
0.5	0.5	0	0.5	8.647	0.728701
0.5	0.5	0	1	8.647	0.84074
0.5	0.5	0	1.5	8.647	0.884595
0.5	0.5	0	2.5	8.647	0.919992
0.5	0.5	0	4	8.647	0.937185
0.5	0.5	0	0.5	8.647	0.728701
0.5	0.5	0	0.5	10	0.716583
0.5	0.5	0	0.5	18	0.665898
0.5	0.5	0	0.5	25	0.6367001
0.5	0.5	0	0.5	30	0.6203001
0.5	0.5	0	0.5	40	0.594175
0.5	0.5	0	0.5	60	0.556813
0.5	0.5	0	0.5	8.647	0.728701
0.5	0.5	1	0.5	8.647	0.595364
0.5	0.5	5	0.5	8.647	0.207886
0.5	0.5	10	0.5	8.647	0.0995574
0.5	0.5	15	0.5	8.647	0.0951682
0.5	0.5	20	0.5	8.647	0.0951349
0.5	0.5	21	0.5	8.647	0.0951348

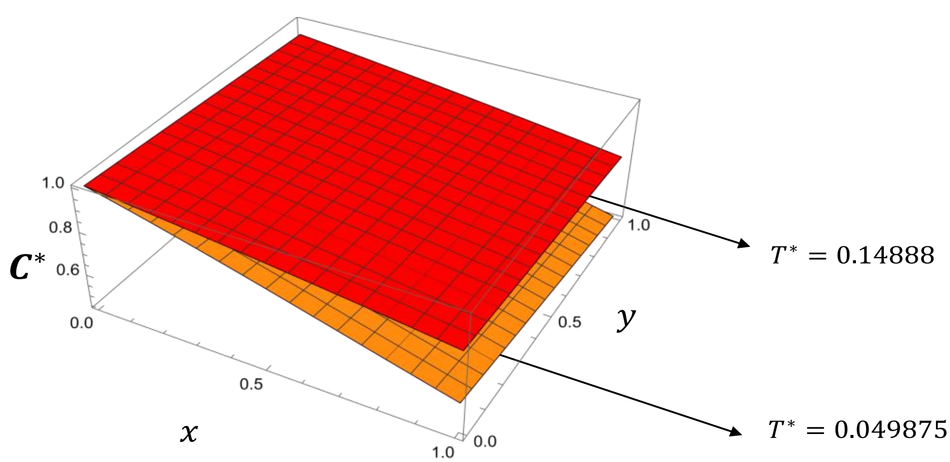

Figure (1): The variation of C^* with time T^* for the values $T^* = 0.049875$ *and* 0,14888, which corresponds to t = 0.5 and 1.5 (day) respectively, $0 \leq x \leq 1(m)$,$0 \leq y \leq 1(m)$, z = 0(m), $Pe = 8.467$.

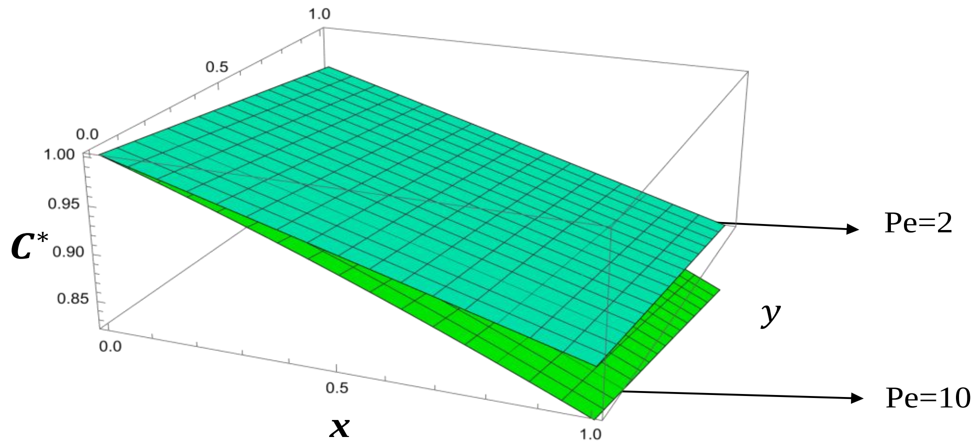

Figure (2): The variation of C^* with Peclet number (Pe), for the values Pe = 2, 10 , $0 \leq x \leq 1(m)$,$0 \leq y \leq 1(m)$, $z = 0$(m), U^*=1.06, C_1^*=0.1 and T^*=0.15.

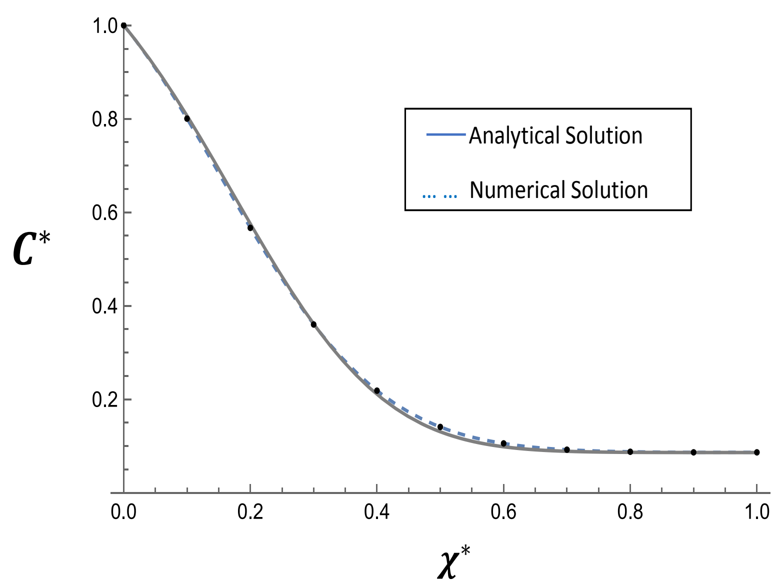

Figure (3): The comparison between the analytical solution (equation (26)) and the numerical solution (equation (36)) for the values $0 \leq \chi^* \leq 1$, $T^* = 0.15$, $Pe = 8.467$, U^*=1.06 and C_1^*=0.1.

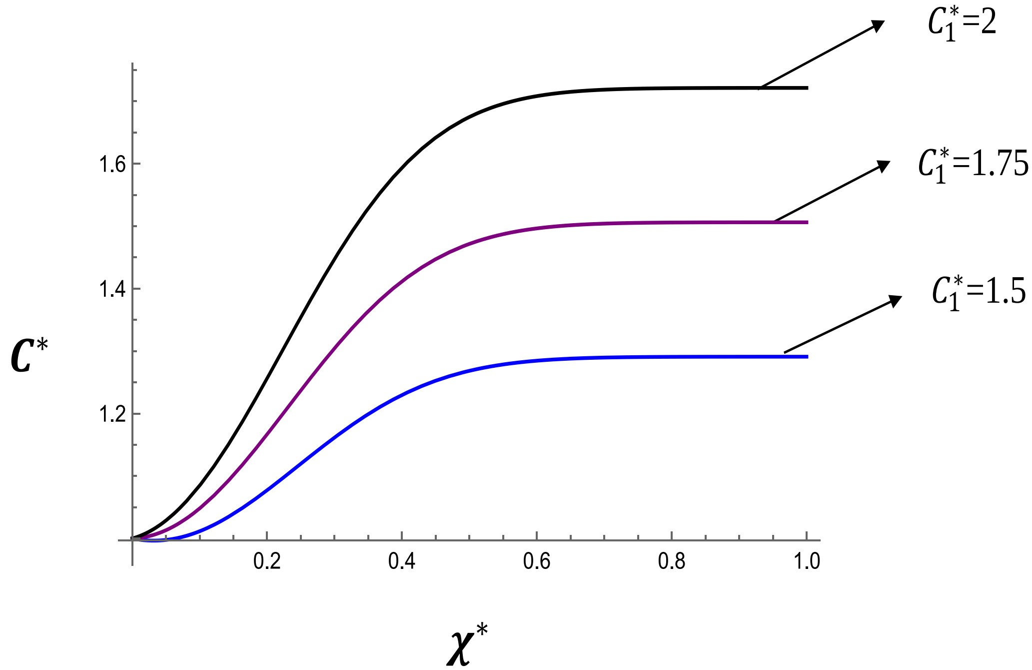

Figure (4): The variation of C^* for the values C_1^*= 1.5, 1.75, 2, $0 \le \chi^* \le 1$, *Pe*=8.467, U^*=1.06 and T^*=0.15.

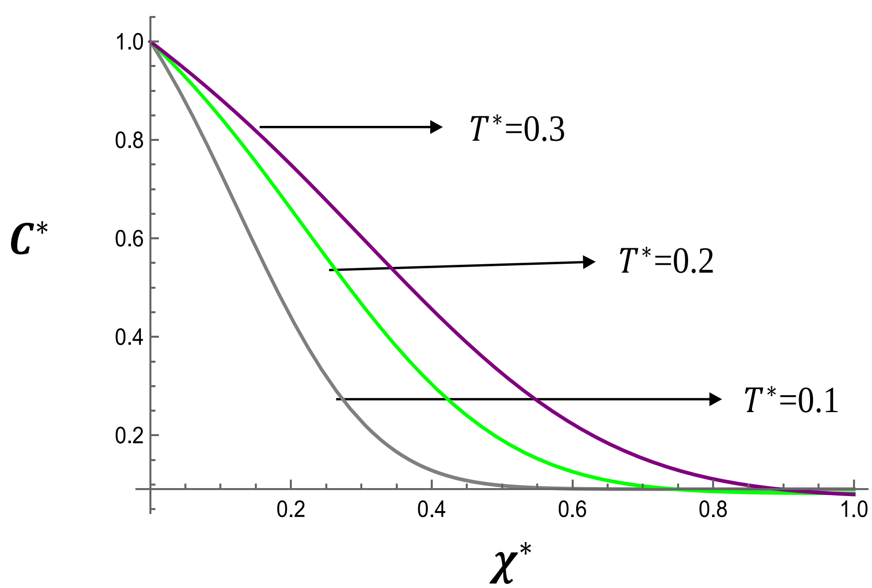

Figure (5): The variation of C^* with T^* at $T^* < {T^*}_0$ for the pulse-type input case for the values $0 \le \chi^* \le 1$, *Pe*=8.467, U^*=1.06, C_1^*=0.1 and ${T^*}_0$=0.5 for T^*=0.1, 0.2 and 0.3

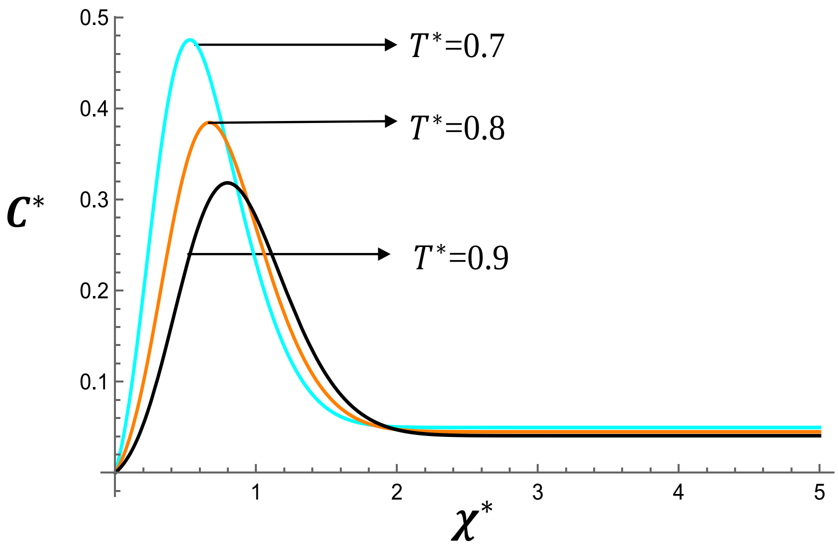

Figure (6): shows the variation of $\boldsymbol{C}^*$ with T^* at $T^* > T^*_0$ for the pulse-type input case for the values $0 \le \chi^* \le 5$, Pe=8.467, U^*=1.06, C_1^*=0.1 and T^*_0=0.5 for T^*=0.7, 0.8 and 0.9.

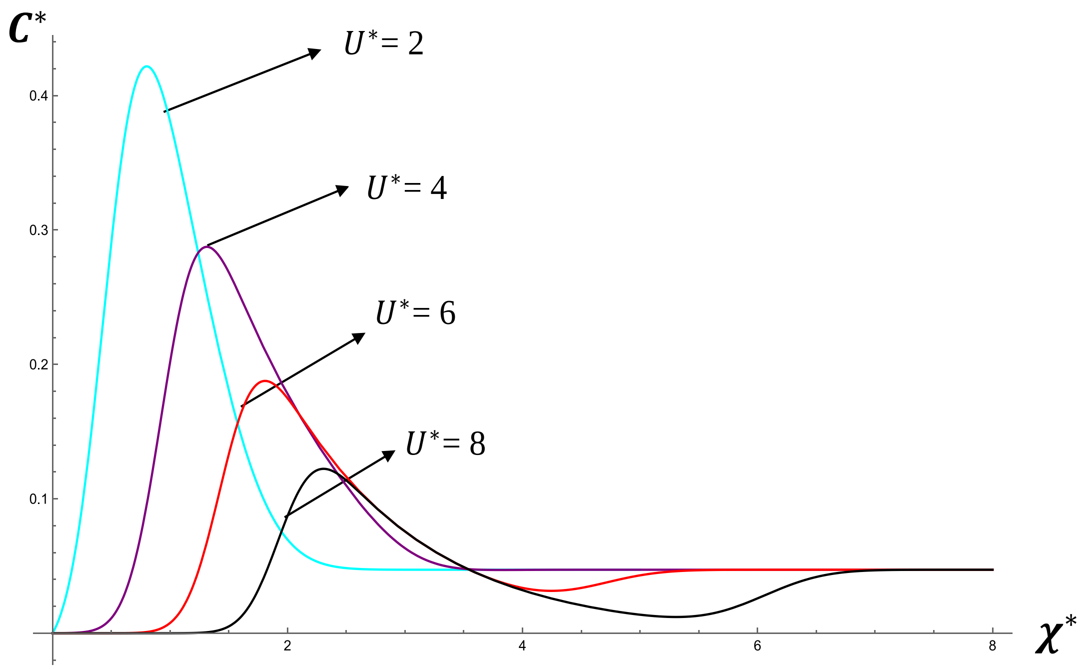

Figure (7): The variation of $C^*$with U^* at $T^* > T^*_0$ for the pulse-type input case for the values $0 \le \chi^* \le 8$, Pe=8.467**,** C_1^*=0.1, T^*=0.75 and T^*_0=0.5 where U^*= 2, 4, 6 and 8.

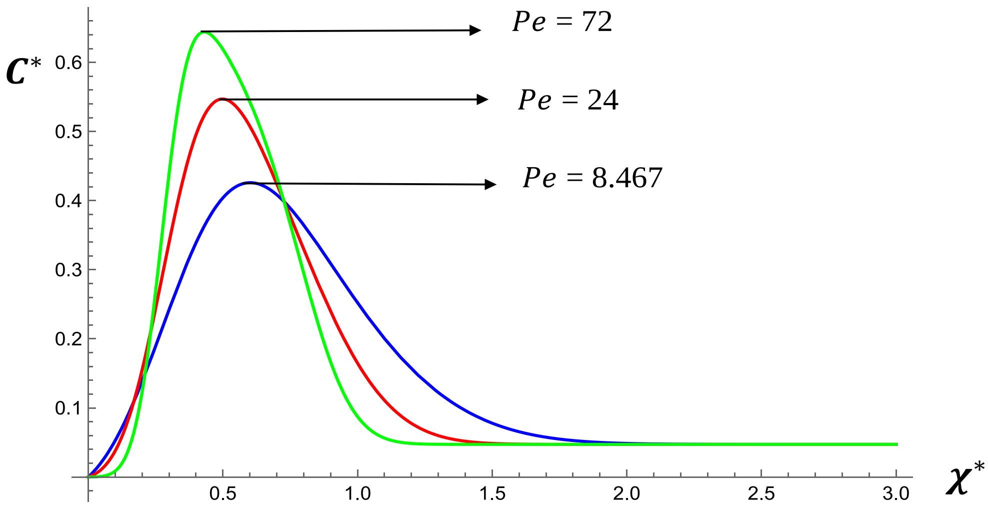

Figure (8): The variation of $\boldsymbol{C}^*$with Pe at $T^* > T^*{}_0$ for the pulse-type input case for the values $0 \le \chi^* \le 3,\ U^* = 1.06,\ C_1^*$=0.1, T^*=0.75 and $T^*{}_0$=0.5 where Pe = 8.467, 24 and 72.

CONCLUSION

The analytical solution is obtained for the three-dimensional advection-dispersion equation describing temporally dependent flow domain through an isotropic semi-infinite homogeneous porous medium by using the Laplace transformation technique. Also, a numerical solution is obtained by using the explicit finite difference method. The usage of dimensionless variables allows this solution to be applicable in a wide variety of cases. When comparing the analytical solution with the numerical solution, we found a very good agreement between them so, the explicit finite difference method is effective and accurate for solving the advection-diffusion equation. Impacts of different parameters controlling the pollutant dispersion have been studied separately with the help of graphs. From **Fig. 1** and **Table 1**, we found that C^* increases as time T^* increases at any point of the domain as expected. From **Fig. 2** and **Table 1**, we found that C^* decreases with the increase of the Peclet number (Pe) at any point of the domain i.e., with the increase of u_0 or the decrease of either D_0 or γ_0. From **Fig. 3** and **Table 1**, we found that for constant values of x, y and increasing values of z, the values of C^* decrease and remain constant as $\chi^* \to \chi^*_\infty$. From **Fig. 4**, we found that near the pumping origin (χ^*=0) where the pollutant concentration of the released water ($C_0^* = 1$) is less than the river's initial pollutant concentration (C_1^*), the effect of C_0^* is dominant, and as χ^*increases, the effect of C_0^* decreases and the effect of C_1^* is dominant. Also, from **Fig. 4**, it is clear that the pollutant concentration takes an intermediate value between C_0^* and C_1^*. This confirms that releasing clean water into the river (i.e. $C_0^* < C_1^*$), decreases the pollutant concentration of the river. Using **Fig. 6**, we can predict with accuracy the time and the position of the peak of the curve which represents the place of accumulation of pollutants in the river, and by doing so we allow for various methods (chemical for example) to be very effective in treating pollution in a relatively small area of the river at a reasonable time.

REFERENCES

Bear, J. (1972). Dynamics of fluids in porous media. New York: Amr.Elsevier.Co.

Bear, J. and Verruijt, A. (1987). Modeling groundwater pollution. In: Modeling groundwater flow and pollution. Theory and applications of transport in porous media, 2.

Bérard, A.; Blais, B. and Patience, G.S. (2020). Experimental methods in chemical engineering: Residence time distribution—RTD. The Canadian journal of Chemical Engineering, 98: 848-867.

Berlin, M. and Suresh, K.G. (2019). Numerical modelling on enhanced mobility of petroleum hydrocarbon in saturated porous media. In: Murali K., Sriram V., Samad A., Saha N. (eds) Proceedings of the Fourth International Conference in Ocean Engineering, 22: 1021-1031.

Borazjani, S.; Kulikowski, D.; Amrouch, K. and Bedrikovetsky, P. (2019). Composition changes of hydrocarbons during secondary petroleum migration (Case study in Cooper Basin, Australia). Geosciences, 9(2):78.

Chaudhary, M.; Thakur, C.K. and Singh, M.K. (2020). Analysis of 1-D pollutant transport in semi-infinite groundwater reservoir. Environ. Earth Sci., 79 (1): 1–23.

Chrysikopoulos, C.V.; Kitandis, P.K. and Roberts, P.V. (1990). Analysis of one-dimensional solute transport through porous media with spatially variable retardation factor. Water Resources Research, 26(3): 437-446.

Crank, J. (1975). The mathematics of diffusion, Oxford Univ. London, 2nd edition.

Dimian, M.; Donia, N.; Wadi, A. and Ibrahim, F. (2014). Impact of El-Rahawy Drain on the water quality of Rosetta Branch of the River Nile, Egypt. International Journal of Environmental Science and Engineering, 5:15-23.

Dimian, M.F.; Wadi, A.S. and Ibrahim, F.N (2013). The effect of added pollutant along a river on the pollutant concentration described by one-dimensional advection diffusion equation. International Journal of Engineering Science and Technology, 5(09):1662-1671.

El Shazely, S. H.; El Gammal, A. H. and Ali, H. M. (2006). Impact of nitrogen discharges on water management in Rosetta River Nile branch. International Commission of Irrigation and Drainage (ICID) Conference At Kuala Lumpur, Malysia.

Esmail, S.; Agrawal, P. and Aly, S. (2020). A novel analytical approach for advection diffusion equation for radionuclide release from an area source. Nuclear Engineering and Technology, 52: 819-826.

Genuchten, M. Th. V. and Alves, W. J. (1982). Analytical solutions of the one-dimensional convective-dispersive solute. U.S.D.A, Tech. Bull. 1661.

Hadhouda, M.Kh. and Hassan, Z.S. (2022). Mathematical model for unsteady remediation of river pollution by aeration. Information Sciences Letters, 11(2): 323-329.

Ibrahim, F.N.; Dimian, M.F. and Wadi, A.S. (2015). Remediation of pollution in a river by unsteady aeration with arbitrary initial and boundary conditions. Journal of Hydrology, 525: 793-797.

Jaiswal, D.K.; Kumar, A.; Kumar, N. and Yadav, R.R. (2009). Analytical solutions for temporally and spatially dependent solute dispersion of pulse type input concentration in one dimensional semi-infinite media. Journal of Hydro- environment research, 2: 254 – 263.

Kumar, A.; Jaiswal, D.K. and Yadav, R.R. (2011). One-Dimensional solute transport for uniform and varying pulse type input point source with temporally dependent coefficients in longitudinal semi-infinite homogeneous porous domain. International Journal of Mathematics and Scientific Computing, 1(2): 56-66.

Leij, F. J.; Skaggs, T. H. and Genuchten, M. Th. V. (1991). Analytical solution for solute transport in three-dimensional semi-infinite porous media. Journal of Water Resources Research, 27(10): 2719-2733.

Manitcharoen, N. and Pimpunchat, B. (2020). Analytical and numerical solutions of pollution concentration with uniformly and exponentially increasing forms of sources. Journal of Applied Mathematics, 2020: 1-9.

Olowe, K.O. and Kumarasamy, M. (2017). Development of the hybrid cells in series model to simulate ammonia nutrient pollution transport along Umgeni River. Environmental Science and Pollution Research, 24: 22967-22979.

Saleh, A.; Ibrahim, F.N. and Hadhouda, M.Kh. (2022). Remediation of pollution in a river by releasing clean water. Information Sciences Letters, 11(1): 127-133.

Savovic, S. and Djordjevich, A. (2012). Finite difference solution of the one-dimensional advection–diffusion equation with variable coefficients in semi-infinite media. International Journal of Heat and Mass Transfer, 55: 4291-4294.

Singh, M. K.; Kumari, P. and Mahato, N. K. (2013). Two-Dimensional solute transport in finite homogeneous porous formations. International Journal of Geology, Earth and Environmental sciences, 3(2):35-48.

Sylvain, T.T.A.; Patrice, E.A.; Marie, E.E.J.; Pierre, O.A. and Hubert, B.G. (2021). Analytical solution of the steady-state atmospheric fractional diffusion equation in a finite domain. Pramana Journal of Physics, 95(1):1-9.

Wadi, A.S.; Dimian, M.F. and Ibrahim, F.N. (2014). Analytical solutions for one-dimensional advection-dispersion equation of the pollutant concentration. Journal of Earth System Science, 123(6): 1317-1324.

Yadav, R.R.; Jaiswal, D.K. and Yadav, H.K. (2010). Analytical solution of one dimensional temporally dependent advection dispersion equation in homogeneous porous media. International Journal of Engineering, Science and Technology, 2(5):141-148.

Yadav, R.R.; Jaiswal, D.K.; Yadav, H.K. and Gulrana (2011). Temporally dependent dispersion through semi-infinite homogeneous porous media: An analytical solution. IJRRAS, 6:158-164.

Yadav, R.R. and Kumar, L.K. (2018). Solute transport for pulse type input point source along temporally and spatially dependent flow. Pollution, 5 (1): 53-70.

Yadav, R.R. and Kumar. L.K. (2021). Analytical solution of two-dimensional conservative solute transport in a heterogeneous porous medium for varying input point source. Environmental Earth Sciences, 80: 327.